Journal of the Ceramic Society of Japan 127 [8] 590-593 2019
DOI http://doi.org/10.2109/jcersj2.19017

JCS-Japan

NOTE

# Structural characterization of mist chemical vapor deposited amorphous aluminum oxide films using water-free solvent

**Zenji YATABE[1,†,‡], Koshi NISHIYAMA[2,‡], Takaaki TSUDA[2] and Yusui NAKAMURA[2,3]**

[1]Priority Organization for Innovation and Excellence, Kumamoto University, Kumamoto 860–8555, Japan
[2]Graduate School of Science and Technology, Kumamoto University, Kumamoto 860–8555, Japan
[3]Kumamoto Phoenics, Kumamoto 862–0901, Japan

**Excellent quality amorphous aluminum oxide ($AlO_x$) thin films have been obtained by atmospheric pressure solution-processed mist chemical vapor deposition (mist-CVD) technique at 400°C using water-free solvent. X-ray fluorescence investigations verified the formation of $AlO_x$ film by the mist-CVD. X-ray diffraction, X-ray photoelectron spectroscopy, ellipsometry and X-ray reflectivity analyses revealed that the synthesized amorphous $AlO_x$ films have bandgap of 6.5 eV, refractive index of 1.64 and mass density of 2.78 g/cm$^3$. These values are comparable to those reported for high-quality amorphous $Al_2O_3$ thin films deposited by atomic layer deposition method.**

©2019 The Ceramic Society of Japan. All rights reserved.

Key-words : Mist chemical vapor deposition, Aluminium oxide, Bandgap

[Received January 9, 2019; Accepted May 20, 2019]

With its high dielectric constant (~9), wide-bandgap (~7 eV) and high breakdown field (~10 MV/cm), amorphous aluminum oxide ($AlO_x$, when $x = 1.5$, i.e., $Al_2O_3$) is an attractive dielectric material for applications as gate insulator and/or surface passivation layers for electrical devices.[1)] Using atomic layer deposition (ALD) method and other vacuum deposition techniques, high-quality $Al_2O_3$ thin films have been reportedly obtained.[2)–8)] Despite the use of pyrophoric precursors such as trimethylaluminium and the typically slow deposition rate (~0.1 nm/cycle),[4)–8)] the ALD technique opened the door for manufacturing III–V metal–oxide–semiconductor field–effect transistors (MOSFETs), because it can provide high-quality $Al_2O_3$ thin films and $Al_2O_3$/III–V interfaces.[1)] One alternative approach to obtain high-quality $Al_2O_3$ thin films is the mist chemical vapor deposition (mist-CVD), which can deposit various metal oxide thin films from relative non-toxic and nonpyrophoric aqueous solution, resulting in relatively simple, low-cost and fast deposition rate under atmospheric pressure.[9)–14)] Recent years have witnessed mist-CVD delivering their promise of high-quality metal oxide thin films and demonstrating their capability as an able replacement for vacuum deposition techniques. For $Al_2O_3$ thin films deposited by mist-CVD, Kawaharamura et al. reported $AlO_x$ thin films having smooth surface[9)] and having highly uniform thickness[10)] grown on 100 mm$^{\varphi}$ substrates. Oh et al.[11)] and Kim et al.[12)] reported $AlO_x$ thin films having breakdown field of approximately 9 MV/cm synthesized by mist-CVD.

For applications as gate dielectric layers in MOS structures, the bandgap of the dielectric material is of particular interest because it dictates the resulting device leakage and breakdown properties. However, to our best knowledge, there have been no reports of systematic determination of bandgap of mist-CVD grown amorphous $AlO_x$ thin films.

In addition, the growth mechanisms of mist-CVD of $AlO_x$ is not fully understood. As oxidizer of mist-$AlO_x$, water is intentionally added to a precursor solvent in general.[9),11),12)] To investigate if water is indeed necessary, we performed deposition of amorphous $AlO_x$ thin films using only methanol ($CH_3OH$, MeOH) solvent (without addition of water to the solvent) and investigated the subsequent growth behavior, chemical properties, crystallinity, bandgap, mass density and refractive index of the deposited films. We confirmed that the obtained values are comparable to those reported for high-quality amorphous $Al_2O_3$ thin films deposited by ALD, thereby demonstrating the efficacy of using mist-CVD in realizing $AlO_x$ films having almost the same properties as those prepared by the more mature ALD method.

In this study, $AlO_x$ films were prepared using a homemade fine-channel-type mist-CVD system. The homemade mist-CVD system was described in detail elsewhere.[13)] Aluminum acetylacetonate [$Al(C_5H_7O_2)_3$, $Al(acac)_3$] was used as the liquid precursor solution (0.06 mol/L), which was diluted in MeOH (99.8% purity). $AlO_x$ films were deposited on boron-doped crystalline silicon (Si) 2-in.-diameter substrates at 400°C with nitrogen carrier gas at a

† Corresponding author: Z. Yatabe; E-mail: yatabe@cs.kumamoto-u.ac.jp
‡ These authors contributed equally to this work.


©2019 The Ceramic Society of Japan

This is an Open Access article distributed under the terms of the Creative Commons Attribution License (https://creativecommons.org/licenses/by-nd/4.0/), which permits unrestricted use, distribution, and reproduction in any medium, provided the original work is properly cited.

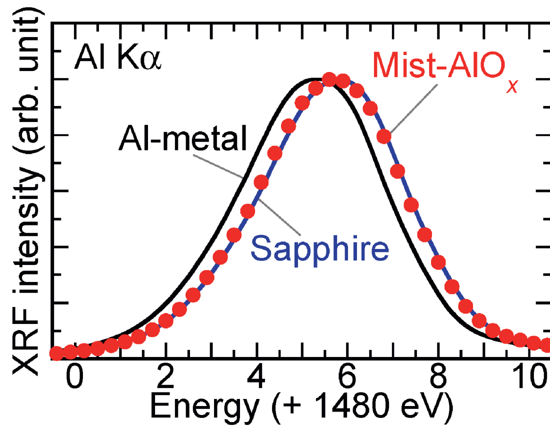


Fig. 1. Al K$\alpha$ XRF spectra of mist-AlO$_x$ (closed symbol) film, reference Al-metal and sapphire substrate (solid line).

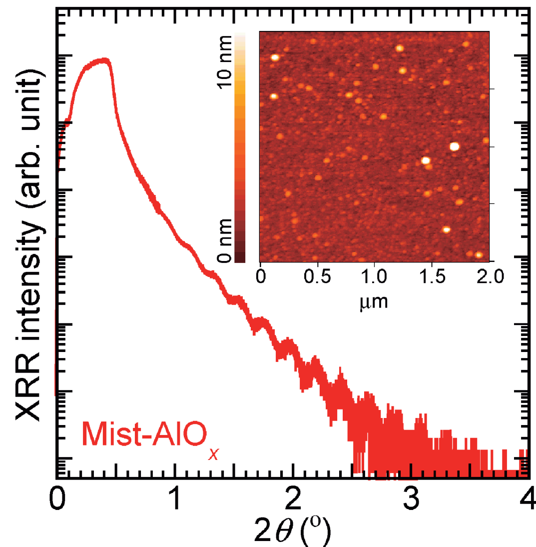


Fig. 2. XRR profiles of mist-AlO$_x$ film deposited on Si substrate. The inset figure shows the mist-AlO$_x$ surface.

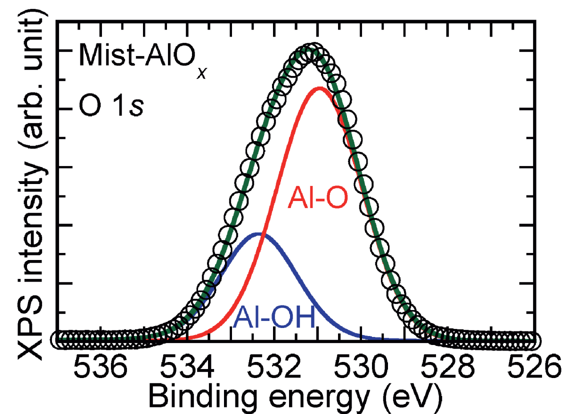


Fig. 3. XPS O 1$s$ core-level spectrum of mist-CVD of AlO$_x$ film at an escape angle of $\theta = 45°$.

flow rate of 3 L/min. Note that all the characterizations were performed on as-deposited samples without undergoing any post-deposition annealing process.

We initially estimated the deposition rate of grown by mist-CVD of AlO$_x$ films using a probe-type step profiler. The deposition rate of mist-CVD is estimated to be 30 nm/min using the present experimental condition. Next, we characterized the chemical properties of as-deposited mist-CVD of AlO$_x$ film with a nominal thickness of 930 nm by X-ray fluorescence (XRF) equipped with a single-crystal spectrometer (Rigaku ZSX Primus II). The Al K$\alpha$ line of mist-CVD AlO$_x$ was compared with that of the reference Al metal with a thickness of 1 mm and that of a crystalline $Al_2O_3$ (sapphire) substrate with a thickness of 430 µm in **Fig. 1**. The Al K$\alpha$ profiles of the mist-CVD of AlO$_x$ and sapphire substrate are shifted 0.38 eV toward the higher energy direction relative to that of the Al metal. The chemical shift of XRF lines is usually interpreted by the effective charges of the X-ray emitting atom.[15),16)] The obtained chemical shift value of 0.38 eV is in good agreement with the reported values 0.37–0.39 eV in going from the Al metal to the $Al_2O_3$.[17),18)] Moreover, the Al K$\alpha$ lines, for both mist-CVD of AlO$_x$ and sapphire substrate, are overlapping. This suggest that the deposited mist-AlO$_x$ is actually nearly stoichiometric (i.e. $x \approx 1.5$).

We also performed X-ray photoelectron spectroscopy (XPS) analyses at an escape angle of 45° using an XPS system (Perkin-Elmer PHI 1600C) equipped with a spherical capacitor analyzer and a monochromated Al K$\alpha$ radiation source ($h\nu = 1486.6$ eV) on mist-CVD AlO$_x$ surface with a nominal thickness of 38 nm. The XPS wide-scan spectra indicate presence of aluminum, oxygen and adventitious carbon while no nitrogen peaks are detected. Since carbon impurities[2),11)] in the AlO$_x$ film and film porosity[12)] can affect the refractive index, ellipsometry and X-ray reflectivity (XRR) measurements were also performed. From the ellipsometry measurement, the refractive index of the mist-CVD of AlO$_x$ with a nominal thickness of 38 nm was estimated to be 1.64, which is close to the values reported for the amorphous $Al_2O_3$ films deposited by ALD.[5)–8)] **Figure 2** shows the XRR profiles of the mist-CVD AlO$_x$ film with a nominal thickness of 38 nm grown on Si substrate. The observation of fringes in the XRR profile indicates the obtained AlO$_x$ film having fairly good surface/interface quality and uniformity of film thickness. The atomic force microscope image of the AlO$_x$ surface, as shown in Fig. 2 (inset), also suggests relatively smooth surface with a root mean square value of 0.94 nm obtained from a $2 \times 2$ µm region. Mass density of the mist-CVD AlO$_x$ film was then estimated to be 2.78 g/cm$^3$ by XRR analysis, which is comparable to the values reported for the amorphous $Al_2O_3$ films deposited by ALD.[6)] These results suggest that the obtained mist-CVD AlO$_x$ is relatively dense as well as having low carbon impurity contamination.

**Figure 3** shows O 1$s$ spectrum of mist-CVD of AlO$_x$ film. Note that XPS profile were calibrated to the adventitious C 1$s$ peak position at a binding energy of 284.8 eV.[19)] The open circles show the measured data and the solid lines represents the pseudo-Voigt function fitting results. The fitting results of O 1$s$ peak exhibited a peak at

531 eV, associated to the Al–O bond and another peak at 532.3 eV, attributed to Al–OH bond.[11),19)] As shown in Fig. 3, Al–O bond has a higher occupation area than Al–OH bond in the mist-CVD of $AlO_x$ film, and the fitted area ratio Al–O and Al–OH were 71 and 29%, respectively. As for ALD of $Al_2O_3$, the residual Al–OH bond were usually observed from XPS measurements.[3)–6)] The fitted area ratio Al–O (71%) and Al–OH (29%) in this work is close to the values reported from the amorphous $Al_2O_3$ thin films prepared by ALD.[3)] Although both ALD and mist-CVD of the films contain Al–OH bond, OH groups may be reduced by post-deposition annealing[3)] or use of higher deposition temperature.[5),9),11)] In fact, using Fourier-transform infrared spectroscopy (FTIR), Kawaharamura et al.[9)] reported the detection of residual Al–OH bond in $AlO_x$ film deposited at 350°C by mist-CVD. In their work, they used $Al(acac)_3$ with mixture of MeOH and water precursor solution. They claimed to have demonstrated dramatic reduction of the residual Al–OH bond in the film deposited 400°C. Although the deposition temperature 400°C is same as the present work, it should be emphasized that we have analyzed the residual Al–OH bond using XPS measurements, which is more surface sensitive that FTIR. Meanwhile, although the origin of the Al–OH bond in mist-CVD of $AlO_x$ is not yet fully understood, we can assume that they originate from the Al atoms that do not oxidized completely and have absorbed moisture from the environment.[11)] Within this line of thinking, it is likely that there are more OH-bonds on the surface region than in the deeper bulk region of the $AlO_x$ film. Using the more surface sensitive XPS method, therefore, relatively higher number of O–H bonds in our sample was detected. Another probable reason is the fact that the precursor solvent used is different between our study and Ref. 9. In this work, we used only MeOH, while on the other hand, mixture of MeOH and water precursor solvent was used in Ref. 9. If the Al–OH bonds indeed originate from the precursor solvent as discussed in Ref. 9, then it can also explain the relatively higher number of O–H bonds detected in our sample.

**Figure 4** shows the X-ray diffraction (XRD) profiles of the mist-CVD $AlO_x$ film with a nominal thickness of 930 nm grown on Si substrate and bare Si substrate. No apparent peak is present apart from that of Si, which indicate that mist-CVD $AlO_x$ film deposited at 400°C has amorphous-phase structure. Ponja et al.[20)] successfully obtained crystalline $\alpha$-$Al_2O_3$ film on quartz substrate via aerosol assisted CVD using $Al(acac)_3$ with MeOH-based precursor solution and the subsequent post-deposition annealing at 1100°C. For the application of $Al_2O_3$ as a gate dielectric in MOSFETs, the amorphous-phase structure is a highly feasible and desirable. Hori et al.[7)] pointed out that microcrystallized $Al_2O_3$ film causes a marked increase in the leakage current of the $Al_2O_3$/GaN MOS structure, which can be problematic especially at high voltage applications. The grain boundaries in the microcrystallized $Al_2O_3$ layer can serve as high-leakage paths and can lead to premature device breakdown.

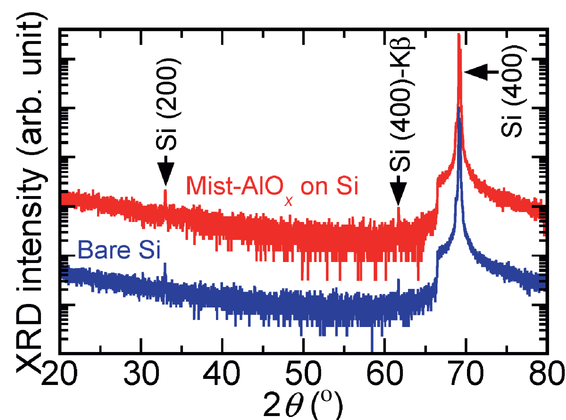


Fig. 4. XRD profiles of mist-$AlO_x$ film deposited on Si substrate and bare Si substrate.

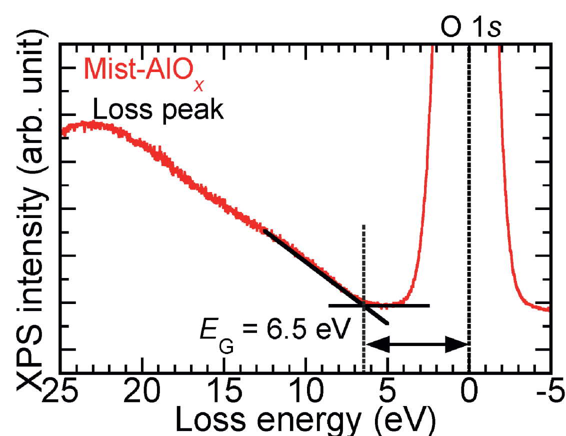


Fig. 5. XPS O 1$s$ core-level and energy loss peaks of mist-CVD of $AlO_x$ film at an escape angle of $\theta = 45°$.

Finally, the bandgap of the mist-CVD $AlO_x$ with a nominal thickness of 38 nm was estimated from the energy-loss peak in the O 1$s$ XPS spectrum.[21)] As shown in **Fig. 5**, the onset of the loss-peak line resulted in $E_G = 6.5$ eV, which is in good agreement with the data reported for amorphous $Al_2O_3$ thin film prepared by ALD. The bandgap of $Al_2O_3$ obtained experimentally from amorphous thin films ranges from 5.9 to 7.0 eV,[4)–7)] which is lower than that of the crystalline $Al_2O_3$ (8.4–8.8 eV).[14),22)] To the best of our knowledge, this is the first report of bandgap of amorphous $AlO_x$ synthesized using mist-CVD. Although further investigation is necessary to characterize electrical properties of the obtained films, the obtained refractive index and mass density are close values to that reported by several groups from their mist-CVD of $AlO_x$ films prepared by similar $Al(acac)_3$-based precursor solution using their own respective mist-CVD system[9)–11)] This significant fact indicates that atmospheric pressure solution-processed mist-CVD technique has high repeatability and universality.

In summary, excellent quality amorphous $AlO_x$ thin films have been obtained by atmospheric pressure solution-processed mist-CVD technique at 400°C using water-free solvent. XRF investigations verified the formation of $AlO_x$ film by the mist-CVD. XRD, XPS, ellipsometry and XRR

analyses revealed that the synthesized amorphous $AlO_x$ films have bandgap of 6.5 eV, refractive index of 1.64 and mass density of 2.78 g/cm$^3$. These values are comparable to those reported for high-quality amorphous $Al_2O_3$ thin films deposited by ALD method, thereby demonstrating the efficacy of using mist-CVD in realizing $AlO_x$ films having almost the same properties as those prepared by the more mature ALD method.

**Acknowledgments** One of the authors (ZY) sincerely thank Professors Tamotsu Hashizume and Masamichi Akazawa of the Research Center for Integrated Quantum Electronics (RCIQE), Hokkaido University, Professor Joel T. Asubar of the Graduate School of Engineering, University of Fukui and Professor Tetsuro Sueyoshi of the Graduate School of Science and Technology, Kumamoto University for their valuable support.

## References

1) Z. Yatabe, J. T. Asubar and T. Hashizume, *J. Phys. D Appl. Phys.*, 49, 393001 (2016).
2) G. He, X. Wang, M. Oshima and Y. Shimogaki, *Jpn. J. Appl. Phys.*, 49, 031502 (2010).
3) Y. Xiang, C. Zhou, E. Jia and W. Wang, *Nanoscale Res. Lett.*, 10, 137 (2015).
4) K. Yoshitsugu, M. Horita, Y. Ishikawa and Y. Uraoka, *Phys. Status Solidi C*, 10, 1426–1429 (2013).
5) S. K. Kim, S. W. Lee, C. S. Hwang, Y.-S. Min, J. Y. Won and J. Jeong, *J. Electrochem. Soc.*, 153, F69–F76 (2006).
6) J. Yang, B. S. Eller, M. Kaur and R. J. Nemanich, *J. Vac. Sci. Technol. A*, 32, 021514 (2014).
7) Y. Hori, C. Mizue and T. Hashizume, *Jpn. J. Appl. Phys.*, 49, 080201 (2010).
8) S. Kaneki, J. Ohira, S. Toiya, Z. Yatabe, J. T. Asubar and T. Hashizume, *Appl. Phys. Lett.*, 109, 162104 (2016).
9) T. Kawaharamura, T. Uchida, M. Sanada and M. Furuta, *AIP Adv.*, 3, 032135 (2013).
10) T. Kawaharamura, *Jpn. J. Appl. Phys.*, 53, 05FF08 (2014).
11) K.-T. Oh, H. Kim, D. Kim, J. H. Han, J. Park and J.-S. Park, *Ceram. Int.*, 43, 8932–8937 (2017).
12) D.-H. Kim, H.-J. Jeong, J. Park and J.-S. Park, *Ceram. Int.*, 44, 459–463 (2018).
13) Z. Yatabe, T. Tsuda, J. Matsushita, T. Sato, T. Otabe, K. Sue, S. Nagaoka and Y. Nakamura, *Phys. Status Solidi C*, 14, 1600148 (2017).
14) T. Uchida, R. Jinno, S. Takemoto, K. Kaneko and S. Fujita, *Jpn. J. Appl. Phys.*, 57, 040314 (2018).
15) G. Leonhardt and A. Meisel, *J. Chem. Phys.*, 52, 6189–6198 (1970).
16) Z. Liu, S. Sugata, K. Yuge, M. Nagasono, K. Tanaka and J. Kawai, *Phys. Rev. B*, 69, 035106 (2004).
17) Y. Gohshi, *Spectrochim. Acta B*, 36, 763–765 (1981).
18) T. Yamamoto, H. Miyauchi, T. Yamamoto and J. Kawai, *Adv. X-ray Chem. Anal. Jpn.*, 41, 177–183 (2010).
19) J. van den Brand, W. G. Sloof, H. Terryn and J. H. W. de Wit, *Surf. Interface Anal.*, 36, 81–88 (2004).
20) S. D. Ponja, I. P. Parkin and C. J. Carmalt, *RSC Adv.*, 6, 102956 (2016).
21) S. Miyzaki, *J. Vac. Sci. Technol. B*, 19, 2212–2216 (2001).
22) R. H. French, *J. Am. Ceram. Soc.*, 73, 477–489 (1990).